

A Numerical Study of Pulsatile Flow Through a Hollow Fiber Cartridge: Growth Factor-Receptor Binding and Dissociation Analysis

Changjiang Zhang

Department of Computer Science
University of Kentucky
Lexington, KY, 40506 USA
czhanb@csr.uky.edu

Wensheng Shen

Department of Computational Science
Suny Brockport
Brockport, NY, 14420 USA
wshen@brockport.edu

M. Fannon

Department of Ophthalmology and Visual Science
University of Kentucky
lexingtont, KY, 40506 USA
mwfann2@email.uky.edu

K. Forsten-Williams

Department of Chemical Engineering
Virginia Tech
Blacksburg, VA, 24601 USA
kfw@vt.edu

Jun Zhang

Department of Computer Science
University of Kentucky
Lexington, KY, 40506 USA
jzhang@cs.uky.edu

Abstract—This paper presents a numerical solution to describe growth factor-receptor binding under flow through hollow fibers of a bioreactor. The multi-physics of fluid flow, the kinetics of fibroblast growth factor (FGF-2) binding to its receptor (FGFR) and heparan sulfate proteoglycan (HSPG) and FGF-2 mass transport is modeled by a set of coupled nonlinear partial differential equations (PDEs) and coupled nonlinear ordinary differential equations (ODEs). A finite volume method is used to discretize the PDEs. The ODEs are solved by a stiff ODE solver CVODE. Overall, second order accuracy in time and space is achieved with the second order implicit Euler scheme. In order to obtain a reasonable accuracy of the binding and dissociation from cells, a uniform mesh is used. To handle pulsatile flow, several assumptions are made including neglecting any entrance effects and an analytical solution for axial velocity within the fibers is

obtained. Qualitative and quantitative analysis are presented. Computational results and experimental measurements are compared and observed to agree quite well, indicating that the simulation model and methods could be used as a complementary and even predictable tool for the study of biochemical reactions in a similar flow environment.

Keywords—CFD; Convective mass transport; FGF-2 binding; Pulsatile flow

I. INTRODUCTION

The binding of fibroblast growth factor-2 (FGF-2) to its cell surface receptor (FGFR) and the role of heparan sulfate proteoglycans (HSPG) in regulating this process for

endothelial cells has been of interest for many years because of their roles in cell signaling and cellular proliferation, processes which important for angiogenesis. Certainly control of these cells which line blood vessels is likely to be important in being able to control tumor growth and wound healing. In the past two decades, with the development of high performance computers, several computational models of FGF-2 binding to its receptor and HSPG have been proposed [1-8]. Nugent and Edelman were among the earliest researchers, developing a simple model, involving these three species, FGF-2, FGFR and HSPG. They measured kinetic binding rate constants experimentally and their results provided a foundation for investigating the complexity of FGF-2 binding. Nugent, Forsten-Williams and coworkers introduced more complexity into their models with dimerization and formation of higher order species. Filion and Popel proposed a model of FGF-2 interactions with cell surface receptors including diffusive transport within the culture dish [7]. Ibrahim and coworkers proposed a simple model for the stepwise assembly of a ternary FGF-2-FGFR-HSPG complex[8]. Not like the previous models for the kinetic assembly of a ternary complex in which binary FGF-2-FGFR or FGFR-HSPG complexes are intermediates, they claimed that FGFR and HSPG are unbound in the absence of FGF-2 ligand, and the availability of FGF-2 results in formation of initial FGF-2-HSPG complexes, which promotes the rapid binding of FGFR and creates a ternary complexes capable of undergoing dimerization and subsequent FGFR activation. Forsten-Williams and coworkers took their model a step further by linking their model to experimental activation of ERK 1/2, an important intracellular signaling pathway component [6].

All previous modeling work is based on culture environment. This paper addresses the competitive binding of FGF-2, FGFR, and HSPG in a flow environment, to mimic blood vessel-like capillaries. The whole model consists of three coupled parts [29]: (1) the media flow part uses the Navier-Stoke equations; (2) the convective mass transport of FGF-2 in the flow uses transport equation; (3) the binding kinetics uses a set of ordinary differential equations. The binding kinetics part is based on Forsten-Williams et al. 2005 model [6].

II. SIMULATION ENVIRONMENT

In order to investigate the quantitative properties of FGF-2 binding, one pass experiments (ie no recycling of the fluid through the cartridge) and simulations have been set up. Fig. 1 is a diagram of the hollow fiber cartridge system used in the experiments. FGF-2 is injected into the left sampling port and the pump is turned on. The fluid is pumped into the cartridge and FGF-2 enters into the 20 hollow-fiber capillaries, which are coated with endothelial cells on the wall. Fluid from the capillaries is pooled in the right

reservoir and collected in tubes approximately every 10 seconds during one pass experiment.

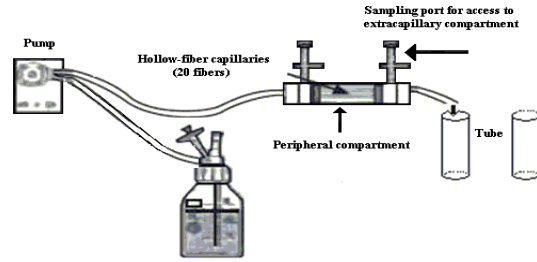


Fig. 1 Hollow fiber cartridge system from FiberCell®

III. MODELING AND NUMERICAL SIMULATION

The geometric model is based on the experimental one and illustrated in Fig 2. The flow is pulsatile, but the simulation cost can be greatly reduced by finding an analytical solution to the velocity, instead of calculating it numerically. The walls of the hollow-fiber capillaries are assumed to be rigid and nonporous. In addition, the following assumptions are made:

(1) All of the 20 hollow-fiber capillaries have the same dimensions, flow, and the cell densities; (2) The flow is steady, axis-symmetrical and laminar. For simplicity, entrance effects are ignored [15]; (3) The fluid is incompressible, Newtonian, viscous and isothermal; (4) The endothelial cells are distributed evenly on the wall of the fiber capillaries and tightly packed.

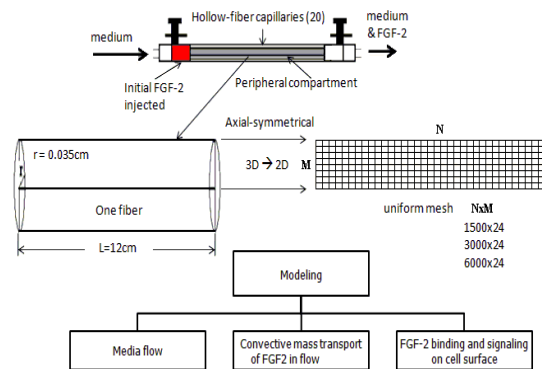


Fig. 2 Diagram of modeling process

The model consists of three coupled parts: (1) the media flow equations; (2) the convective mass transport equations of FGF-2 in the flow; (3) the competitive binding kinetics equations [6][29].

A. The MediaFlow Equations

Because of the axis-symmetry of the fiber capillaries,

the model can be simplified from 3D to 2D. The governing equations of the model are given by [11][22][29]

The mass conservation equation

$$\frac{\partial u}{\partial x} + \frac{v}{r} + \frac{\partial v}{\partial r} = 0 \quad (1)$$

the radial momentum equation

$$\rho\left(\frac{\partial v}{\partial t} + u\frac{\partial v}{\partial x} + v\frac{\partial v}{\partial r}\right) + \frac{\partial p}{\partial r} = \mu\left(\frac{1}{r}\frac{\partial v}{\partial r} + \frac{\partial^2 v}{\partial x^2} + \frac{\partial^2 v}{\partial r^2} - \frac{v}{r^2}\right) \quad (2)$$

the axial momentum equation

$$\rho\left(\frac{\partial u}{\partial t} + u\frac{\partial u}{\partial x} + v\frac{\partial u}{\partial r}\right) + \frac{\partial p}{\partial x} = \mu\left(\frac{1}{r}\frac{\partial u}{\partial r} + \frac{\partial^2 u}{\partial x^2} + \frac{\partial^2 u}{\partial r^2}\right) \quad (3)$$

If these equations are restricted to only fully developed region of the flow, (1) reduces to

$$\frac{v}{r} + \frac{\partial v}{\partial r} = \frac{1}{r}\frac{\partial(rv)}{\partial r} = 0 \text{ so } v \equiv 0 \text{ and } \frac{\partial p}{\partial r} \equiv 0. \text{ Eq. (2)}$$

can be eliminated. Eq. (3) reduces to

$$\rho\frac{\partial u}{\partial t} + \frac{\partial p}{\partial x} = \mu\left(\frac{1}{r}\frac{\partial u}{\partial r} + \frac{\partial^2 u}{\partial r^2}\right) \quad (4)$$

In (4), ρ is the density, u is the axial velocity, p the dynamic pressure, and μ is the viscosity of the media. For a Newtonian incompressible flow, μ is a constant. Eq. (4) is the simplified form on which the classical solution for fully developed steady and pulsatile flow is based.

If the tube is assumed to be rigid, the velocity of u is a function of r and t only, and pressure p is a function of x and t only, that is, $u = u(r, t)$, $p = p(x, t)$. For oscillatory flow, if the steady and oscillatory parts of velocity and pressure are identified by subscripts “s” and “ Φ ”, respectively, to isolate the oscillatory flow problem, we write

$$u(r, t) = u_s(r) + u_\phi(r, t) \text{ and } p(x, t) = p_s(x) + p_\phi(x, t)$$

Substituting these into (4), we obtain

$$\left\{\frac{\partial p_s}{\partial x} - \mu\left(\frac{1}{r}\frac{\partial u_s}{\partial r} + \frac{\partial^2 u_s}{\partial r^2}\right)\right\} + \left\{\rho\frac{\partial u_\phi}{\partial t} + \frac{\partial p_\phi}{\partial x} - \mu\left(\frac{1}{r}\frac{\partial u_\phi}{\partial r} + \frac{\partial^2 u_\phi}{\partial r^2}\right)\right\} = 0 \quad (5)$$

Suppose pressure gradient is $\frac{\partial p}{\partial x} = k_s + k_\phi(t)$

Eq. (5) can be separated into the steady and oscillatory parts. For steady equation

$$\frac{\partial p_s}{\partial x} - \mu\left(\frac{1}{r}\frac{\partial u_s}{\partial r} + \frac{\partial^2 u_s}{\partial r^2}\right) = 0 \quad (6)$$

The solution is $u_s = \frac{k_s}{4\mu}(r^2 - R^2)$, and

$$u_s(0) = \frac{-k_s R^2}{4\mu} = \hat{u}_s, \text{ and } k_s = \frac{-4\mu\hat{u}_s}{R^2}$$

The volumetric flow rate

$$q_s = \int_0^R u_s 2\pi r dr = \frac{-k_s \pi R^4}{8\mu} = \frac{\pi R^2}{2} u_s(0)$$

For oscillatory equation

$$\mu\left(\frac{1}{r}\frac{\partial u_\phi}{\partial r} + \frac{\partial^2 u_\phi}{\partial r^2}\right) - \rho\frac{\partial u_\phi}{\partial t} = k_\phi(t) \quad (7)$$

Let $k_\phi(t) = k_s e^{i\omega t} = k_s (\cos\omega t + i\sin\omega t) = k_{\phi R} + ik_{\phi I}$ and

$$u_\phi(r, t) = U_\phi(r) e^{i\omega t}$$

$$\text{Eq. (7) becomes } \frac{1}{r}\frac{dU_\phi}{dr} + \frac{d^2 U_\phi}{dr^2} - \frac{i\alpha}{R^2} U_\phi = \frac{k_s}{\mu} \quad (8)$$

where, $\alpha = \sqrt{\frac{\rho\omega}{\mu}} R$. Combining boundary conditions,

$$U_\phi(R) = 0 \text{ and } |U_\phi(0)| < \infty, \text{ the solution is}$$

$$U_\phi = \frac{ik_s R^2}{\mu\alpha^2} \left(1 - \frac{J_0(\varsigma)}{J_0(\Lambda)}\right) = U_{\phi R} + iU_{\phi I}$$

Therefore,

$$u_\phi(r, t) = \frac{ik_s R^2}{\mu\alpha^2} \left(1 - \frac{J_0(\varsigma)}{J_0(\Lambda)}\right) e^{i\omega t} = \hat{u}_s \left\{ \frac{-4}{\Lambda^2} \left(1 - \frac{J_0(\varsigma)}{J_0(\Lambda)}\right) e^{i\omega t} \right\} \quad (9)$$

where, $\Lambda = \left(\frac{i-1}{\sqrt{2}}\right)\alpha$, $\varsigma = \Lambda \frac{r}{R}$, and $J_0(z)$ is Bessel functions of the first kind of order zero.

$$u_\phi(r, t) = \frac{-k_s R^2}{4\mu} \left\{ \left(1 - \frac{r^2}{R^2}\right) - \frac{i\alpha^2}{16} \left(3 - \frac{4r^2}{R^2} + \frac{r^4}{R^4}\right) \right\} e^{i\omega t} \quad (10)$$

When oscillatory flow at low frequency, that is

$$\alpha = \sqrt{\frac{\rho\omega}{\mu}} R < 1.0, \text{ the second part can be ignored.}$$

$$\text{Eq.(10) becomes } u_\phi(r, t) = \frac{-k_s R^2}{4\mu} \left(1 - \frac{r^2}{R^2}\right) e^{i\omega t}$$

Let $k_\phi(t) = k_{\phi R}$, then

$$u(r, t) = u_s(r) + u_\phi(r, t) = \hat{u}_s \left(1 + \cos\omega t\right) \left(1 - \frac{r^2}{R^2}\right) \quad (11)$$

Eq. (11) is used as a special case analytical solution of u during the simulation, and Eq. (10) can be used as a general solution to any pulsatile pressure gradient function.

B. The Mass Transport Equations

The mass transport equation for FGF-2 consists of two mechanisms, *convection* and *dissipation*. The convection describes transport of local components along the streamlines of the flow. The dissipation describes diffusive transport of components due to concentration gradient. The mass must be conserved. In the existence of chemical reaction, the coupling of mass transport and chemical kinetics in a circular pipe can be described by the following equation [29]:

$$\frac{\partial \phi}{\partial t} + \frac{1}{r}\frac{\partial(ru\phi)}{\partial r} + \frac{\partial(v\phi)}{\partial x} = \frac{1}{r}\frac{\partial}{\partial r}(rK_d\frac{\partial \phi}{\partial x}) + \frac{\partial}{\partial x}(K_d\frac{\partial \phi}{\partial x}) + F(\phi) \quad (12)$$

where ϕ is the concentration of FGF-2, u and v are the axial and radial components of velocity, K_d is the molecular diffusion coefficient, and F is the rate of change due to kinetic transformations for FGF-2. If we assume the flow in the fiber is fully developed, (12) can be simplified as (13).

$$\frac{\partial \phi}{\partial t} + \frac{1}{r}\frac{\partial(ru\phi)}{\partial r} = \frac{1}{r}\frac{\partial}{\partial r}(rK_d\frac{\partial \phi}{\partial x}) + \frac{\partial}{\partial x}(K_d\frac{\partial \phi}{\partial x}) + F(\phi) \quad (13)$$

The boundary conditions of (13) are

$$\frac{\partial \phi}{\partial r} = f(t, x) \text{ at } r = R, \quad \frac{\partial \phi}{\partial r} = 0 \text{ at } r = 0 \quad (14)$$

A transient solution is pursued in the current simulations. To achieve second order time accuracy, a quadratic backward approximation for the time derivative term is used. In (13), the convective term needs special treatments for stability. To enhance numerical stability as well as maintain second order spatial accuracy, a deferred correction numerical strategy is used [11][29], which is a combination of the first order upwind differencing and the second order central differencing. The diffusive terms are discretized by the central difference method. The equation is solved by Stone's strong implicit procedure (SIP) [12].

C. Binding Kinetics Equations

The binding kinetics involves a series of molecular activities, including FGF-2 binding to its receptors, HSPG, some intermediate complexes or dimers, and internalization. The model from Forsten-Williams et al. [6] is adopted. Nine chemical reactions and ten species are involved [6][29].

The computational model is expressed as a set of ODEs in Table 1[6][7] and some key parameters used are in Table 2.

Table 1 Equations included in the computational model

1	$\frac{dR}{dt} = -k_{onFR}FR + k_{offFR}C + k_{offFHR}T - k_cRG - k_{int}R + k_{int}R_0$
2	$\frac{dC}{dt} = k_{onFR}FR - k_{offFR}C - k_cCH - k_cC^2 + 2k_{uc}C_2 - k_{int}C$
3	$\frac{dC_2}{dt} = \frac{k_c}{2}C^2 - k_{uc}C_2 - k_{intD}C_2$
4	$\frac{dT}{dt} = k_cRG + k_cCH - k_{offFHR}T - k_cT^2 + 2k_{uc}T_2 - k_{int}T$
5	$\frac{dT_2}{dt} = \frac{k_c}{2}T^2 - k_{uc}T_2 + k_{intD}T_2$
6	$\frac{dH}{dt} = -k_{onFH}FH + k_{offFH}G + k_{offFHR}T - k_cCH - k_{int}H + k_{int}H_0$
7	$\frac{dG}{dt} = k_{onFH}FH - k_{offFH}G - k_cRG - k_cG^2 + 2k_{uc}G_2 - k_{int}G$
8	$\frac{dG_2}{dt} = \frac{k_c}{2}G^2 - k_{uc}G_2 - k_{intD}G_2$
9	$\nu \frac{dF}{dt} = -k_{onFR}FR + k_{offFR}C + k_{offFHR}T - k_{onFH}FH + k_{offFH}G - k_{onN}F + k_{offN}N$
10	$\frac{dN}{dt} = k_{onN}F - k_{offN}N$

Key: F-FGF-2, R-FGFR, H-HSPG, C-FGF-2-FGFR complex, C_2 -FGF-2-FGFR dimer, G-FGF-2-HSPG complex, G_2 -FGF-2-HSPG dimer, T-FGF-2-FGFR-HSPG complex, T_2 -FGF-2-FGFR-HSPG dimer, N-Non-specific bound of FGF-2

Table 2 Parameter values used in simulation

Parameter	Value	Meaning(Reference)
k_{onFR}	$4.2 \times 10^8 \text{ M}^{-1} \text{ min}^{-1}$	Association rate constant for FGF-2 and FGFR(26)

k_{offFR}	0.79 min^{-1}	Dissociation rate constant for FGF-2 and FGFR(26)
k_{onFH}	$1.2 \times 10^8 \text{ M}^{-1} \text{ min}^{-1}$	Association rate constant for FGF-2 and HSPG(26)
k_{offFH}	1.37 min^{-1}	Dissociation rate constant for FGF-2 and HSPG (7)
k_{offFHR}	0.038 min^{-1}	Dissociation rate constant for FGF-2, HSPG and FGFR (26)
k_c	$0.001 (\#/cell)^{-1} \text{ min}^{-1}$	coupling rate constant (27)
k_{uc}	1.0 min^{-1}	uncoupling rate constant (27)
k_{int}	0.005 min^{-1}	Internalization rate constant(26)
k_{intD}	0.078 min^{-1}	Internalization rate constant for dimers(26)
k_{onN}	$2.67 \times 10^{13} (\#/cell) \text{ M}^{-1} \text{ min}^{-1}$	Association rate constant for non-specific binding of FGF-2(Fit value)
k_{offN}	0.0001 min^{-1}	Dissociation rate constant for nonspecific binding of FGF-2(assumed)
R_0	$10^4 \#/cell$	Initial FGFR density(3,7,28)
H_0	$10^6 \#/cell$	Initial HSPG density(3,7, 28)
D	$1.57 \times 10^{-10} \text{ m}^2/\text{s}^A$	FGF-2 Diffusivity at 37°C(7)
μ	$0.001 \text{ Pa} \cdot \text{s}^B$	Viscosity of aqueous solution
ρ	$1000 \text{ kg}/\text{m}^3$	Density of aqueous solution

^AFilion & popel (2004), but aqueous solution we used has different viscosity^B.

IV. IMPLEMENTATION DETAILS

A. The Concentration of FGF-2 at Inlet

To more closely link the simulations to the experimental model system, several additional assumptions were made. In our experimental system, FGF-2 is injected into a reservoir and then distributed into the individual capillary fibers. The FGF-2 concentration in the reservoir is assumed to decrease gradually as: $\Phi_n = \Phi_{n-1} \times (\nu - \Delta\nu) / \nu$ where ν is the volume of the reservoir, $\Delta\nu$ is the volume of fluid flowing into the fibers at each pulse, Φ_{n-1} is the

previous concentration and Φ_n is the current concentration of FGF-2 in the reservoir.

B. The Mass of FGF-2 Bound

FGF-2 binding is assumed to occur only on the cell surfaces and the total FGF-2 bound either specifically (FGFR or HSPG) or nonspecifically within the fibers is calculated with the following algorithms. The number of molecules of FGF-2 specifically bound within the fibers is determined as

$$F_n = F_{n-1} + N_f \times K_{gf} \sum_{i=1}^N \{(1+k_{int}) \times (C_i^n - C_i^{n-1} + T_i^n - T_i^{n-1} + G_i^n - G_i^{n-1}) + 2 \times (1+k_{intD}) (C_{2,i}^n - C_{2,i}^{n-1} + T_{2,i}^n - T_{2,i}^{n-1} + G_{2,i}^n - G_{2,i}^{n-1})\}$$

where, K_{gf} is the grid factor. C , T , G are the number of FGF-2 complexes and C_2 , T_2 and G_2 are the number of FGF-2 dimers (refer to Table 1). k_{int} is the internalization rate constant of complexes and k_{intD} is the internalization rate constant of dimers. n is the n th time step, N_f is the number of fibers in the cartridge.

The mass of FGF-2 specifically bound is calculated by $M_F = F_n \times 18/6.022 \times 10^{23} \times 10^{12}$ (ng)

The number of molecules of FGF-2 nonspecifically bound within the fibers is determined as

$$B_n = B_{n-1} + N_f \times K_{gf} \sum_{i=1}^N (B_i^n - B_i^{n-1})$$

The mass of nonspecific FGF-2 bound is calculated by $M_B = B_n \times 18/6.022 \times 10^{23} \times 10^{12}$ (ng)

C. The Mass of FGF-2 Flowing Through the Fibers

The mass of FGF-2 moving through the fibers at location x in axial direction in Δt can be integrated by

$$M_{FGF}(x) = N_f \times 2\pi \int_0^{\Delta t} \int_0^R u(r,t) \Phi(r,t,x) r dr dt$$

Numerically, it can be estimated by

$$M_{FGF}(x) = N_f \times \sum_{i=1}^M \pi (r_i^2 - r_{i-1}^2) u_i(x) \Delta t \Phi_i(x)$$

where Δt is the time step, $u_i(x)$ is the axial velocity and $\Phi_i(x)$ is the concentration of FGF-2 on the i th grid in radial direction and at location x in axial direction. M is the number of grids in radial direction.

V. SIMULATION RESULTS

A. Mesh Size Impact

The impact of mesh size on the simulation results was evaluated. Three different mesh sizes 1500x24, 3000x24, 6000x24, were tested with all other parameters held constant. Fig. 3 is the comparison of FGF-2 flowing out of the fibers using different mesh sizes.

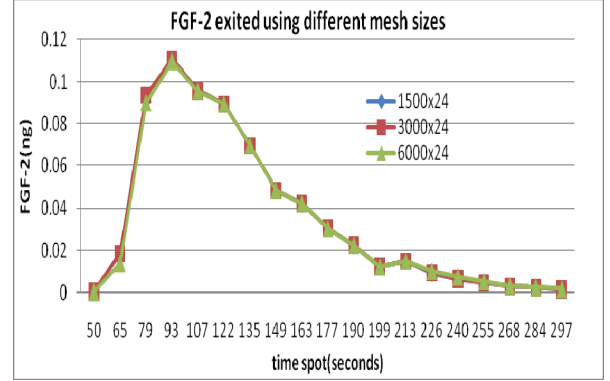


Fig. 3 Comparison of FGF-2 flowing out of the fibers using different mesh sizes

There are only very slight differences when different mesh sizes were used and the binding properties on the cell surface are also essentially unchanged (data not shown). We conclude that the mesh size has little impact on the results within the range that we investigated. We therefore used the coarsest grid and, unless stated, was the 1500x24 mesh size.

B. The Flow Rate and the Amount of Binding

We hypothesized that higher flow rates would result in less specific and nonspecific binding due to lower residence time in the cell environment. Table 3 shows the quantitative relationship between flow rate and binding. Identical simulation parameters except the flow rate were used. Fig. 4 shows the relationship between flow rate and the amount of nonspecific binding, which seems to be a linear relationship for our system. Fig. 5 shows the amount of FGF-2 exiting the system as a function of time and flowrate.

Table 3 The relationship between flow rate and binding

Flow rate (ml/min)	FGF-2 exit (ng)	Specific binding (ng)	Nonspecific binding (ng)
0.6	3.96	0.0016	1.48
0.7	4.12	0.0012	1.31
0.8	4.26	0.0009	1.19
0.9	4.37	0.0007	1.08

Initial FGF-2 injected 5.47ng, diffusivity $1.57 \times 10^{-10} \text{ m}^2/\text{s}$, heparinase treated cells, total simulation time 643s.

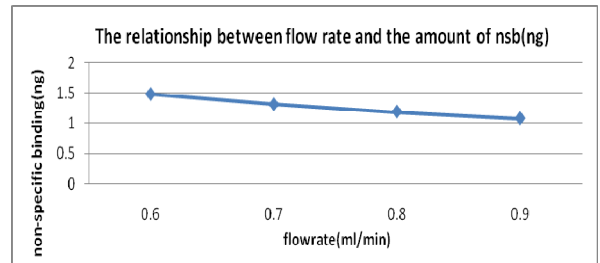


Fig. 4 The relationship between flow rate and the amount of non-specific binding of FGF-2

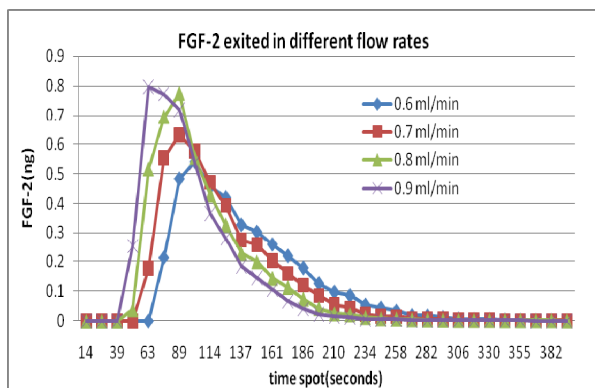


Fig. 5 The amount of FGF-2 exited in different flow rates

C. The Diffusivity and the Amount of Binding

Generally, larger diffusivity or smaller viscosity values will lead to more molecules of FGF-2 dissipating toward the wall, where cells are located. More binding will likely occur resulting in less FGF-2 exiting. Several simulations were conducted with the same parameters except the diffusivity or viscosity to find out the quantitative relationship between the two, as shown in Table 4.

Table 4 The relationship between diffusivity and binding

Diffusivity (cm ² /s)	Viscosity (cP)	FGF-2 exit (ng)	Specific binding (ng)	Nonspecific binding (ng)
5.22x10 ⁻⁷	3 ^A	0.72	0.13	0.049
1.57x10 ⁻⁶	1 ^B	0.55	0.22	0.088
1.75x10 ⁻⁶	0.89 ^C	0.53	0.23	0.093
2.18x10 ⁻⁶	0.72 ^D	0.48	0.25	0.103

Initial FGF-2 injected 0.92ng, flow rate 0.63ml/min, total simulation time 715s. ^Ablood at 25°C, ^BThe solution we used, ^Cwater at 25°C, ^DFilion & Popel(2004)[7]

It is clear that larger diffusivity or smaller viscosity values did lead to have more specific FGF-2 bound to FGFR and HSPG but more nonspecific binding of FGF-2 as well. Diffusivity also affected the profile of FGF-2 outflow (data not shown).

VI. CONCLUSION AND FUTURE WORK

A simulation program has been developed specifically for the simulation of FGF-2 cell binding within the FiberCell[®] Bioreactor Systems, an *in vitro* flow cell culture system. Some interesting simulation results have been obtained. We found: (1) the amount of FGF-2 specifically cell bound is dominated by HSPG coupling (data not shown); (2) the amount of specific and nonspecific binding of FGF-2 is proportional to the diffusivity of the solution and roughly linear proportional to the flow rate; (3) different flow rates or diffusivities will affect the profile of

FGF-2 outflow and the distribution of FGF-2 bound on the wall along the fiber at different time points.

Next, multi-pass simulation will be conducted to find out long term binding properties and more species will be introduced into the model to simulate the impact of alternative species, e.g., some drugs may be added into the fluid along with the FGF-2 to study its influence on FGF-2 binding. The model has to be adjusted and a parallel algorithm may have to be introduced. In order to increase the simulation accuracy, some assumptions or algorithms will be improved.

In conclusion, we have developed a simulation package to describe flow through a capillary with reactive walls. We have applied the model to FGF-2 binding to endothelial cells but the package could be easily modified to accommodate a multitude of similar biological systems.

ACKNOWLEDGMENT

Financial support from the National Institutes of Health (NIH-HL086644) is gratefully acknowledged.

REFERENCES

- [1] M. A. Nugent, E. R. Edelman, Kinetics of basic fibroblast growth factor binding to its receptor and heparan sulfate proteoglycan: A mechanism for cooperativity, *Biochemistry* **31**,1992, pp8876-8883.
- [2] C. J. Dowd, C. L. Cooney, and M. A. Nugent, Heparan sulfate mediates bFGF transport through basement membrane by diffusion with rapid reversible binding, *The Journal of Biological Chemistry* **274**,1999, pp5236-5244.
- [3] M. Fannon, K. E. Forsten, and M. A. Nugent, Potentiation and inhibition of bFGF binding by heparin: a model for regulation of cellular response, *Biochemistry* **39**, 2000, pp1434-1445.
- [4] K. E. Forsten, M. Fannon, and M. A. Nugent, Potential mechanisms for the regulation of growth factor binding by heparin, *Journal of Theoretical Biology* **205**, 2000, pp215-230.
- [5] M. A. Lovich and E. R. Edelman, Computational simulations of local vascular heparin deposition and distribution, *American Journal of Physiology Heart and Circulatory Physiology* **271**,1996, H2014-2024.
- [6] K. Forsten-Williams, C. C. Chua, and M. A. Nugent, The kinetics of FGF-2 binding to heparan sulfate proteoglycans and MAP kinase signaling, *Journal of Theoretical Biology* **233**, 2005, pp483-499.
- [7] R. J. Filion, A. S. Popel, A reaction-diffusion model of basic fibroblast growth factor interactions with cell surface receptors, *Annals of Biomedical Engineering* **32**, 2004, pp645-663.
- [8] O. A. Ibrahim, et al, Kinetic model for FGF, FGFR, and proteoglycan signal transduction complex assembly, *Biochemistry* **43**, 2004, pp4724-4730.
- [9] P. N. Brown, et cl, VODE: A variable-coefficient ODE solver, *SIAM J. Sci. Stat. Comput.* Vol. 10, **5**, 1989, pp1038-1051.
- [10] S. V. Patankar, Numerical heat transfer and fluid flow, The McGraw-Hill Company, Inc., New York, 1980.

- [11] J. H. Ferziger and M. Peric, Computational methods for fluid dynamics, Springer, Berlin, Germany, 1999.
- [12] H. L. Stone, Iterative solution of implicit approximations of multidimensional partial equations, *SIAM J. Numer. Anal.* **5**, 1968, pp530-558.
- [13] J. Folkman, R. Langer, R. J. Linhardt, C. Haudenschild, and S. Taylor, Angiogenesis inhibition and tumor regression caused by heparin or a heparin fragment in the presence of cortisone. *Science* **221**, 1983, pp719-725.
- [14] K. E. Forsten, and D. A. Lauffenburger, Probability of autocrine ligand capture by cell-surface receptors: implications for ligand secretion measurements. *J. Comp. Bio.* **1**, 1994, pp15-23.
- [15] R. W. Hornbeck, Laminar flow in the entrance region of a pipe, *Applied Science Research* **13**, 1964, pp224-232.
- [16] H.S. Lew, Y.C. Fung, Entry length into blood vessels at arbitrary Reynolds number, *J. of Biomechanics*, **3**, 1970, pp23-38.
- [17] A. Horowitz, E. Tkachenko, and M. Simons, Fibroblast growth factor-specific modulation of cellular response by syndecan-4, *Journal of Cell Biology*, **157**, 2002, pp715-725.
- [18] B. M. Johnson, P. R. Johnston, S. Corney, and D. Kilpatrick, Non-Newtonian blood flow in human right coronary arteries: steady state simulations, *Journal of Biomechanics*, **37**, 2004, pp709-720.
- [19] B. N. Kholodenko, O. V. Demin, G. Moehren, and J. B. Hoek, Quantification of short term signaling by the epidermal growth factor receptor, *Journal of Biological Chemistry*, **274**, 1999, pp30169-30181.
- [20] R. LeVeque, Finite volume methods for hyperbolic problems, *Cambridge University Press*, Cambridge, UK, 2002.
- [21] S. Elhadj, etc. Chronic pulsatile shear stress impacts synthesis of proteoglycans by endothelial cells: effect on platelet aggregation and coagulation, *J. of cellular Biochemistry* **86**, 2002, pp239-250.
- [22] M. Zamir, The Physics of Pulsatile Flow, Springer-Verlag New York, Inc., 2000.
- [23] M. J. Ott and B. J. Ballermann, Shear stress-conditioned, endothelial cell-seeded vascular grafts: improved cell adherence in response to in vitro shear stress, *Surgery*, **117**, 1995, pp334-339.
- [24] B. B. Riley, M. P. Savage, B. K. Simandl, B. B. Olwin, and J. F. Fallon, Retroviral expression of FGF-2 (bFGF) affects patterning in chick limb bud, *Development*, **118**, 1993, pp95-104.
- [25] G. V. Sperinde and M. A. Nugent, Heparan sulfate proteoglycans control bFGF processing in vascular smooth muscle cells. *Biochemistry*, **37**, 1998, pp13153-13164.
- [26] G. V. Sperinde, and M. A. Nugent. Mechanisms of fibroblast growth factor 2 intracellular processing: A kinetic analysis of the role of heparan sulfate proteoglycans. *Biochemistry* **39**, 2000, pp3788-3796.
- [27] B. S. Hendriks, L. K. Opresko, H. S. Wiley, A. Wells, D.A. Lauffenburger, Quantitative analysis of HER2-mediated effects on HER2 and epidermal growth factor receptor endocytosis: distribution of homo- and heterodimers depends on relative HER2 levels. *J. Biol. Chem.* **278**, 2003, pp23343-23351.
- [28] D. E. Johnson, and L. T. Williams. Structural and functional diversity in the FGF receptor multigene family, *Adv. Cancer Res.* **60**, 1993, pp1-41.
- [29] W. Shen, C. Zhang, M. Fannon, K. Forsten-Williams, Jun Zhang, A computational model of FGF-2 binding and HSPG regulation under flow, *IEEE Transactions on BioMed. Eng.*, in press.